



Development of Linear Vernier Hybrid Permanent Magnet Machine for Wave Energy Converter

N. Arish*, V.Teymoori

Faculty of Electrical and Computer Engineering, Semnan University, Semnan, Iran

PAPER INFO

Paper history:

Received 21 January 2020

Received in revised form 10 February 2020

Accepted 21 March 2020

ABSTRACT

Keywords:

Wave Energy Converter
Permanent Magnet Machine
Vernier Machine
Halbach Array
Linear Machine
Finite Element Method

Today, due to the limited supply and rapid consumption of fossil fuels, transitioning towards renewable energy supplies has become more important than ever.. The purpose of this paper is to present a new linear permanent magnet vernier machine structure which is designed to capture wave energy and improve the performance of the prototype vernier machine. By halving the proposed vernier machine, amending gear ratio and changing the shape of permanent magnet (PM) and teeth, the performance of the proposed vernier machine increases compared to the prototype vernier machine. This novelty causes the proposed vernier machine to be lighter, more economical and more efficient than the prototype vernier machine. Moreover, the main parameters of the proposed vernier machine compared to the prototype vernier machine are improved, so that in the proposed vernier machine, induced voltage, PM flux and thrust force are increased by 30, 68 and 27% respectively. In addition, the ripple of thrust force is reduced by 5%, and the self-inductance is diminished by 55%. All analyses have been performed in the same conditions with the finite element method using Ansys Maxwell software.

doi: 10.5829/ije.2020.33.05b.12

1. INTRODUCTION

Renewable energies are classified into solar, marine, wind energy and etc [1]. Among the various sub-categories of marine energy, wave energy is the most important and popular energy, because of its high reliability, convenient accessibility, predictability and high power density [2, 3]. To use marine energy, we need energy converters. The electric machines are the main parts of these converters. Energy converters which are used in the marine are classified into two types of rotary and linear converters. One of the newest structures is the Permanent Magnet (PM) converters that are capable of generating more force and power due to PM excitation [4]. Converters are designed in different structures, each of which has its own unique features so that each wave energy converter is designed and built according to installation location and type of operation. In general, the structure of the PM convertors is classified into five main categories: point absorber, oscillating water column, oscillating wave surge, pressure differential, and overtopping converter [5]. PM converters can be

designed in flat or tubular structures which using magnetorheological (MR) fluids and dampers, reduces the vibration and makes control easier [6, 7]. In the tubular structure, the translator can be outside and inside and the magnets can be mounted on both the translator and the stator [8, 9]. Using magnets on the translator makes the construction complex and also increases the likelihood of demagnetization. On the other hand, the use of a magnet on the stator in electric machines with long stator will increase the magnet size, weight and the cost of its construction. The linear vernier machine is one of the newest electric PM machines which is used in wave energy converters due to its high power output at low speeds which is because of the presence of multiple magnetic poles. This type of machine in addition to its unique features has downsides such as low power factor and high leakage flux; which engineers have designed new structures to improve these drawbacks. In literature [10, 11], by reducing the size of the magnets and changing the structure of the teeth and PM, the magnetic circuit has been unbalanced which reduced the leakage flux and improved the machine performance. Moreover,

*Corresponding Author Email: Nima.Arish@gmail.com (N. Arish)

in [12, 13], by applying high-temperature superconductor (HTS), leakage fluxes have been removed and the performance of the machines have been improved due to zero relative permeability of this type of material. Authors in [14, 15] improved performance of the proposed machines by correct selection of PM orientation and teeth shape. The purpose of this paper is to present a new linear permanent magnet vernier machine structure for capturing wave energy which is designed based on the prototype permanent magnet vernier machine [16] and improves the performance of the prototype vernier machine. So that by halving, size and weight of the proposed machine have been reduced. In addition, by keeping the volume of magnets constant and transferring them from the halbach structure to the skew in two different magnetic directions and also, by amending the magnetic gear ratio and changing the structure of teeth, performance of the proposed machine has been increased. The rest of the paper is organized as follows: The structure and function are given in section 2. Section 3 presents the finite element method (FEM) analysis of the main parameters for the proposed and prototype vernier PM machines. The conclusions are also given in Section 4.

2. STRUCTURE AND FUNCTION

The proposed linear PM vernier converter is applied at the beach in the oscillating wave surge mode as shown in Figure 1. The arm in the water transfers the wave energy to the translator by means of mechanical gearboxes, which results in the translator movement and induced voltage generation. The proposed vernier hybrid PM machine is designed based on the prototype vernier PM machine, Figures 2 (a) and 2 (b) illustrate the structure of the proposed and prototype machines, respectively. As it is obvious, the proposed vernier hybrid PM machine consists of a stator and a one-way translator and the prototype vernier PM machine consists of two stators and a two-way translator. As shown in Figure 2, the coils are centrally mounted in both structures and both machines consist of three separate phases so that in the proposed vernier hybrid PM machine, each phase consists of 2 coils and in the prototype vernier PM machine each phase consists of 4 coils. In addition, the translator is divided into three phases which there is not any connection between them and they are autonomous. This feature causes the value of mutual inductance to be approximately zero which it leads to excellent fault-tolerant capability in both machines. The core material of both machines is made of iron and the coils are copper and the magnets used in both machines are of the NdFe35 type. The magnets are mounted in the halbach form, on the translator of the prototype vernier PM machine and

on the stator of the proposed vernier hybrid PM machine. Moreover, they are mounted in the stator of the proposed vernier hybrid PM machine diagonally and magnetized in two different magnetic directions, so as to magnetize the magnets towards the stator teeth, which can direct the produced flux to the teeth and then to the stator yoke. The structure of the magnets with halbach array for producing the sinusoidal flux must be such as to satisfy the following formula [17]:

$$w_v + 2w_h < \tau_s \quad (1)$$

$$w_h \leq w_v \quad (2)$$

where, w_v , w_h and τ_s are the width of the middle part of halbach PM, the width of side part of halbach PM and pole pitch, respectively. In both models, halbach array consists of three parts, such that the width of the middle magnet is larger than the width of the two other magnets, which produces an asymmetric magnetic flux and the field produced on one side is stronger than the other. This feature generates a more sinusoidal flux over the air gap. The magnetic direction of the larger magnet is towards the stator teeth and the direction of the smaller magnets is towards each other. For new design in linear permanent magnet machine, must consider this formula [18]:

$$P_{\text{fluxeff}} = |P_t - P_{\text{PM}}| = 1 \quad (3)$$

where, P_t is the number of active translator's teeth, P_{PM} the number of pole pairs on the stator and P_{fluxeff} the pole pair number of the effective magnetic flux which is modulated by the translator's teeth. As can be seen, the proposed vernier hybrid PM machine is designed based on considering $P_{\text{fluxeff}} = 1$:

$$P_{\text{fluxeff}} = |P_t - P_{\text{PM}}| = 1 \begin{cases} \text{proposed-machine} = P_{\text{fluxeff}} = |18-17| = 1 \\ \text{prototype-machine} = P_{\text{fluxeff}} = |24-23| = 1 \end{cases} \quad (4)$$

The gear ratio (G_r) in electric machines which is one of the most important design parameters is as follows [18]:

$$G_r = \frac{P_t}{|P_t - P_{\text{PM}}|} = \begin{cases} \text{proposed-machine} = G_r = \frac{18}{|18-17|} = 18 \\ \text{prototype-machine} = G_r = \frac{24}{|24-23|} = 24 \end{cases} \quad (5)$$

The base of the vernier machine is on a magnetic gearbox, and since the number of its magnetic poles is high, with the smallest translator movement, the flux over the air gap varies considerably. That is why the vernier machine is capable of generating high power at low speeds.

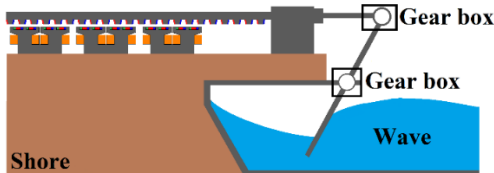


Figure 1. The proposed linear PM vernier converter applied at the beach

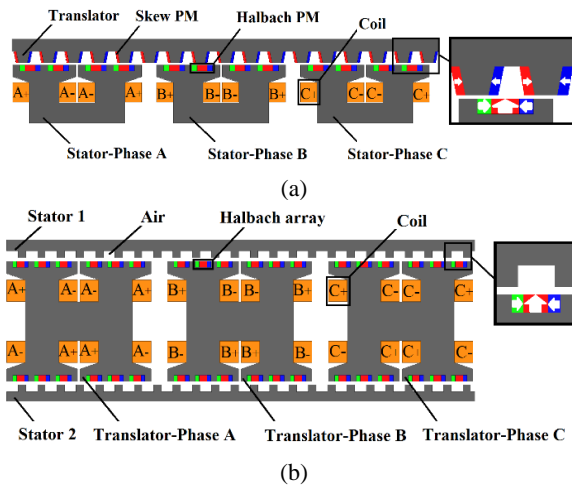
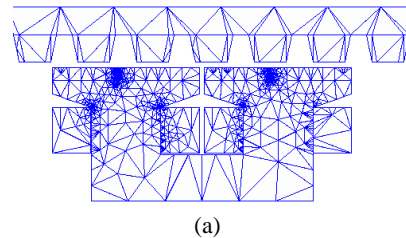


Figure 2. The structure of the proposed and prototype machines, (a) Proposed vernier hybrid PM machine, (b) Prototype vernier PM machine

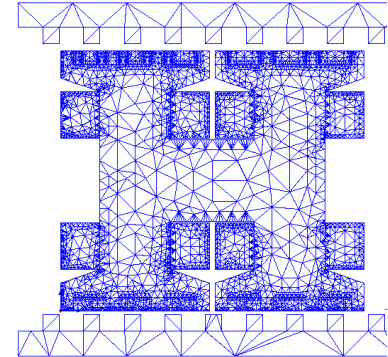
3. FINITE ELEMENT METHOD

Maxwell Ansys can be able to analyse electrical machine in transient and magnetostatic mode based on the FEM. The FEM analysis is a strong method for accurate design and modelling of electrical devices. Indeed, all linear and nonlinear properties of the PM material, core material, and geometric description can be considered by using a type of formulation namely $T\cdot\Omega$, $A\cdot V$, E and H formulation [19, 20]. The Maxwell equations written in each of these formulas are essentially the same, but the solutions of the relevant partial differential equation cannot be the same [21]. Electromagnetic and transient behaviour of the electrical machines have been accurately calculated by solving the Maxwell equation based on the A-V method. The electromagnetic performances for both of the models are analyzed and compared at the same conditions. These comparisons have been done in terms of induced voltage, PM flux, self-inductance, mutual inductance, thrust force, detent force and power factor. Mesh diagrams for models are shown in Figure 3.

Moreover, the main design parameters of the proposed vernier hybrid PM machine are shown in Figure 4 and their values are given in Table 1.



(a)



(b)

Figure 3. Mesh diagrams for both of the machines, (a) Proposed vernier hybrid PM machine, (b) Prototype vernier PM machine

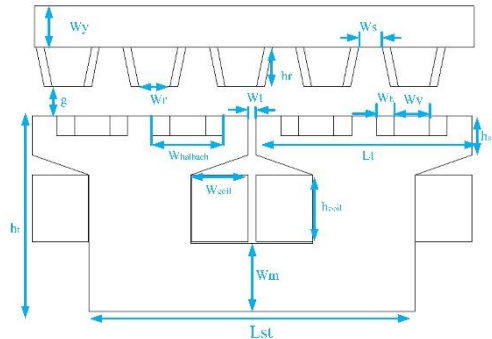


Figure 4. The main design parameters of the proposed vernier hybrid PM machine

3. 1. Magnetic Field Distribution

Figure 5 shows the distribution of the flux lines at the no-load state in the same position for the prototype and the proposed vernier machine. As shown, the flux lines in the halbach array is asymmetric and the flux lines in the phase of both machines are independent. Moreover, the flux density of the proposed vernier hybrid PM machine is much higher than the flux density of the prototype vernier PM machine.

The reason for the higher density of the flux in the proposed vernier hybrid PM machine is that, in this machine, the fluxes are closed in a loop, but in the prototype vernier PM machine, the flux path is divided into two different loops and directions. Besides, the

TABLE 1. Main design parameters of the proposed vernier hybrid PM machine

Items	Unit	Proposed machine
ws	mm	6
wh	mm	4.5
wv	mm	9
g	mm	2
wy	mm	10.5
wm	mm	17.5
wr	mm	8
hr	mm	10
hs	mm	10
ht	mm	50
Lst	mm	55
wcoil	mm	14.5
hc	mm	17
whalbach	mm	18

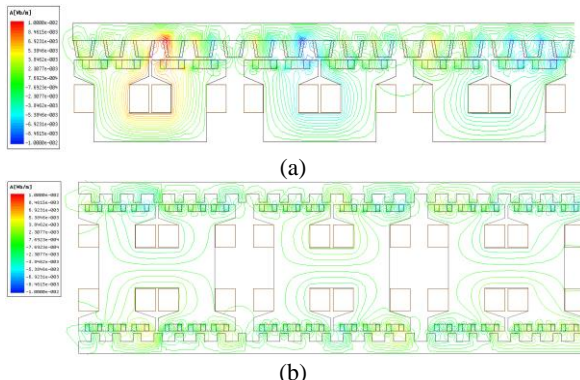


Figure 5. The distribution of the flux lines at no-load state, (a) Proposed vernier hybrid PM machine, (b) Prototype vernier PM machine

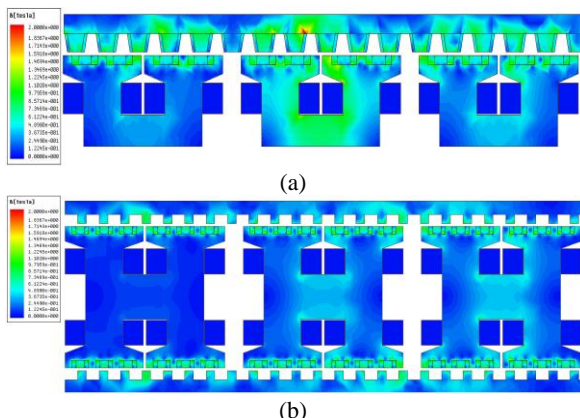


Figure 6. The flux density distribution at full load state, (a) Proposed vernier hybrid PM machine, (b) Prototype vernier PM machine

magnetic direction of the skew magnets on the stator causes the flux produced by the magnets to enter the yoke with a higher density. Figure 6 shows the flux density distribution at full load state. As it can be seen, the density of the magnetic field in the proposed vernier hybrid PM machine is higher than the prototype vernier PM machine and the maximum value for both machines is less than 2 T, indicating that the machines are not saturated.

3. 2. PM Flux and Induced Voltage

The induced voltage in the vernier machine can be obtained using the following equation [17]:

$$\text{EMF} = \frac{d\psi}{dt} \quad (6)$$

According to (6), the PM flux and the induced voltage are proportional to each other. Figures 7 (a) and (b) show the PM flux at no-load state for the proposed vernier hybrid PM machine and the prototype vernier PM machine, respectively. The root mean square (RMS) amounts of PM flux in the proposed vernier hybrid PM machine and the prototype vernier PM machine are 0.049 Wb and 0.029 Wb respectively, indicating that the PM flux in the proposed vernier hybrid PM machine is increased by 39%. Since the value of PM flux in the proposed vernier hybrid PM machine is higher than the prototype vernier PM machine, the induced voltage in the proposed vernier hybrid PM machine is also higher than the prototype vernier PM machine. Figures 7 (c) and (d) depict the induced voltage at no-load state for the proposed vernier hybrid PM machine and the prototype vernier PM machine, respectively. In addition, the peak values of the induced voltage in the proposed and prototype vernier PM machine are 34 V and 26 V respectively, showing that the induced voltage in proposed vernier hybrid PM machine is raised by 25%. This increase is due to the increased flux density in the teeth and yoke of the proposed vernier hybrid PM machine.

3. 3. Self-inductance and Mutual Inductance

In the vernier PM machine, the self-inductance and mutual inductance can be obtained by modifying the phase main flux with the phase current [23]:

$$\left\{ L_{bb} = \frac{\psi_{b-lb} - \psi_{b-0}}{I_b}, M_{ba} = \frac{\psi_{a-lb} - \psi_{a-0}}{I_b} \right\} \quad (7)$$

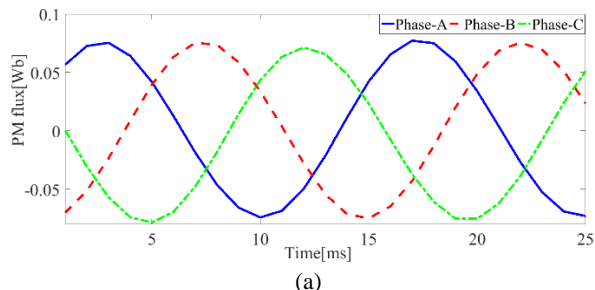
where, L_{bb} is the self-inductance of phase b, and M_{ba} is the mutual inductance of phases b and a. ψ_{b-lb} is the main flux of phase b in phase b current. Furthermore, ψ_{a-lb} is the main flux of phase a in phase b current, and ψ_{b-0} and ψ_{a-0} are the fluxes of phases a and b at no-load state. Figures 8 (a) and (b) show the self-inductance of the proposed vernier hybrid PM machine and the prototype

vernier PM machine respectively. Moreover, Figures 8 (c) and (d) show the mutual inductance of the proposed vernier hybrid PM machine and the prototype vernier PM machine respectively. Inductance depends on the position of the translator and coil. The self-inductances in the proposed and prototype vernier PM machine are 16 mH and 35 mH, respectively. It means that self-inductance in the proposed vernier hybrid PM machine is diminished by 55%. In addition, the mutual inductances in both of the machines are close to zero as the phases are separated. Mutual inductance is one of the most important parameters in the field of reliability as it indicates the magnetic coupling between coils. Moreover, it is crucial to have very low mutual inductance because by this situation, when the fault occurs in one coil, this fault cannot affect on other coils. Therefore, the fault-tolerant capability in the proposed vernier hybrid PM machine improves.

3.4. Power Factor Power factor is one of the main characteristics of the electric machines. The low power factor of the vernier machine is one of its well-known features, and many structures have been proposed to improve and enhance it. Figure 9 shows a diagram of the phasor irrespective of the stator resistance. The power factor ($\cos \Theta$) depends on the angle between U_s and E . Assuming that the current i_d is zero, the power factor can be obtained from the following equation [24]:

$$PF = \frac{1}{\sqrt{\frac{L_s i}{\psi} + 1}} \quad (8)$$

where, L_s , i and ψ are the synchronous inductance, phase current and the PM flux, respectively. Following (8), to increase the power factor, the inductance and PM flux should be decreased and increased respectively. As stated above, the synchronous inductance in the proposed vernier hybrid PM machine is lower than that of the prototype vernier PM machine, and the PM flux in the proposed vernier hybrid PM machine is higher than PM flux in the prototype vernier PM machine, so the power factor in the proposed vernier hybrid PM machine is higher than the prototype vernier PM machine.



(a)

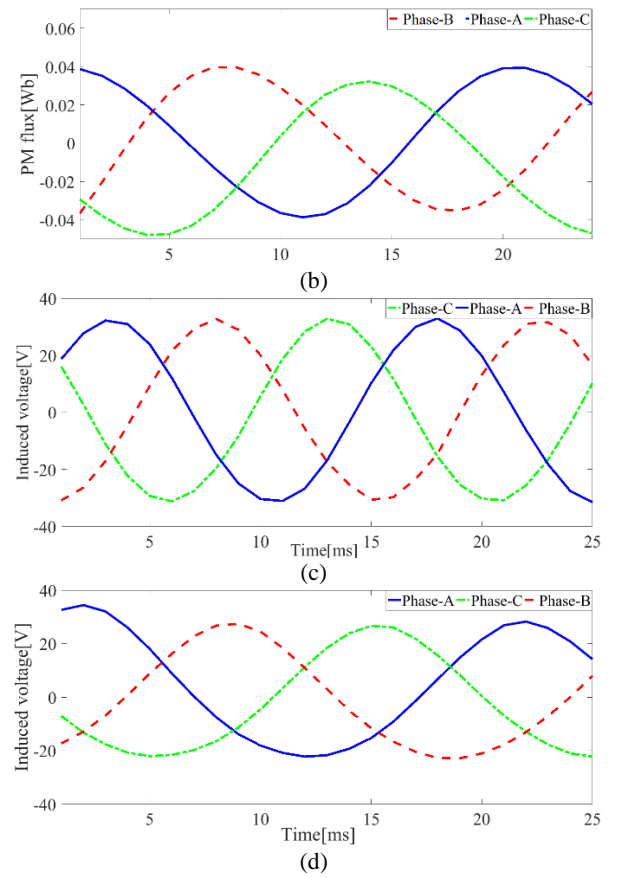
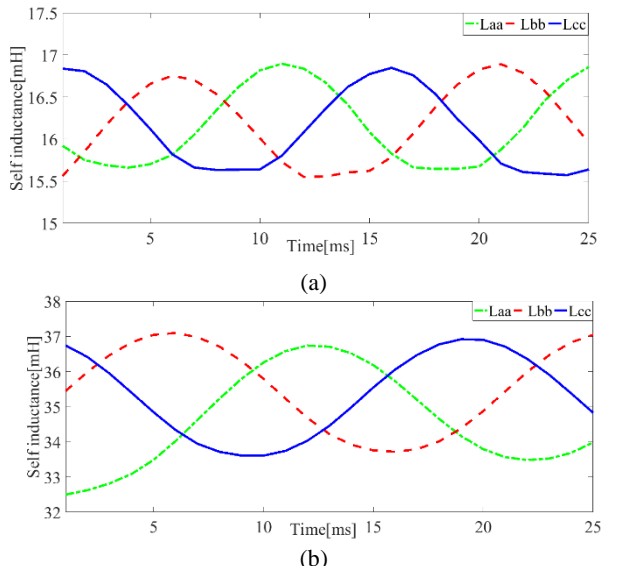


Figure 7. Comparison of the PM flux and induced voltage at no-load state for both machines, (a) PM flux of the proposed vernier hybrid PM machine, (b) PM flux of the prototype vernier PM machine, (c) Induced voltage of the proposed vernier hybrid PM machine, (d) Induced voltage of the prototype vernier PM machine



(a)

(b)

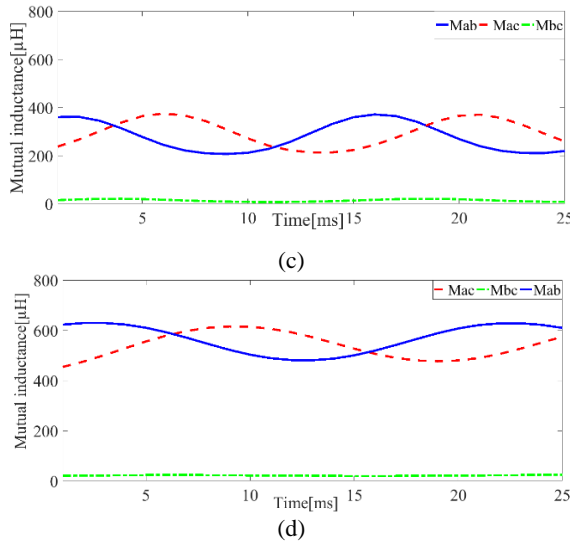


Figure 8. Comparison of self inductance and mutual inductance for both machines, (a) Self inductance of the proposed vernier hybrid PM machine, (b) Self inductance of the prototype vernier PM machine, (c) Mutual inductance of the proposed vernier hybrid PM machine, (d) Mutual inductance of the prototype vernier PM machine

3.5. Thrust Force and Detent Force For vernier machines, it is not possible to accurately measure the thrust force during translator motion due to vibration and friction. However, the following formula can be used to calculate the thrust force [23]:

$$F_{\text{thrust}} = F_{\text{detent}} + F_{\text{ele}} \quad (9)$$

According to Equation (9), the thrust force consists of detent and electromagnetic forces, where F_{ele} is the force generated by the magnetic field and the coil current.

The detent force is a destructive factor that its excess causes the machine to ripple and shake. The detent force in a linear machine is equivalent to the cogging torque in a rotating machine. The detent force is generated from the sum of the slot effect and end effect. It is a very complicated task to calculate the slot effect and end effect separately as they affect each other. There are many ways to reduce the detent force and ripple of the thrust force of the vernier machine, the most important of which

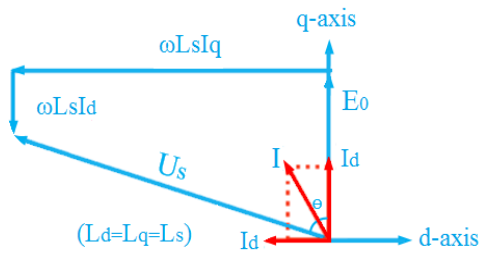


Figure 9. A diagram of the phasor

is to skew the teeth and the magnets, and select an appropriate gear ratio [20, 21]. Figures 10 (a) and (b) show the detent force and thrust force for the proposed and prototype vernier PM machines, respectively. As can be seen, the thrust force in the proposed vernier hybrid PM machine is much higher than the prototype vernier PM machine so that the average thrust forces for the proposed and prototype vernier PM machines are 2300 N and 1800 N, respectively.

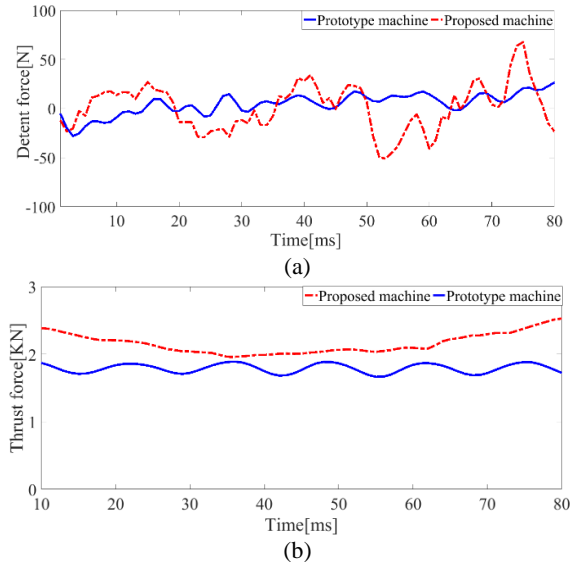
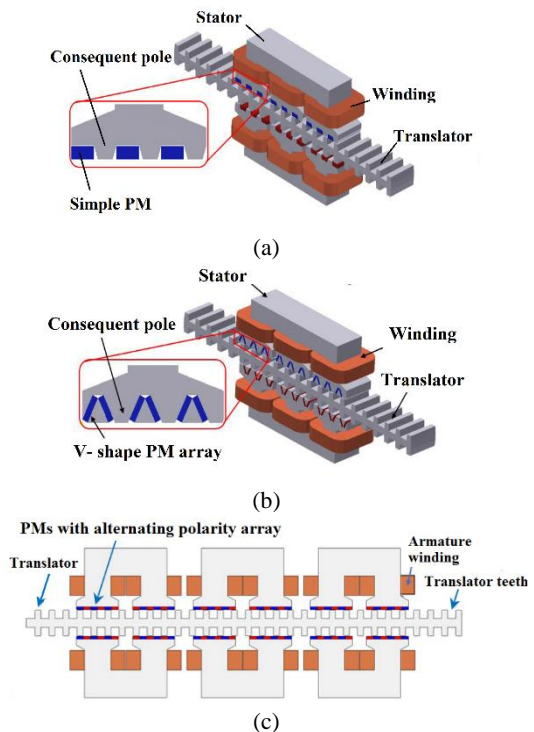


Figure 10. Comparison of detent force and thrust force for both machines, (a) Detent force, (b) Thrust force



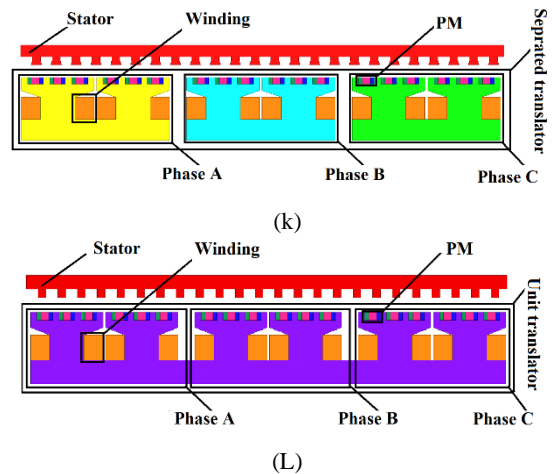
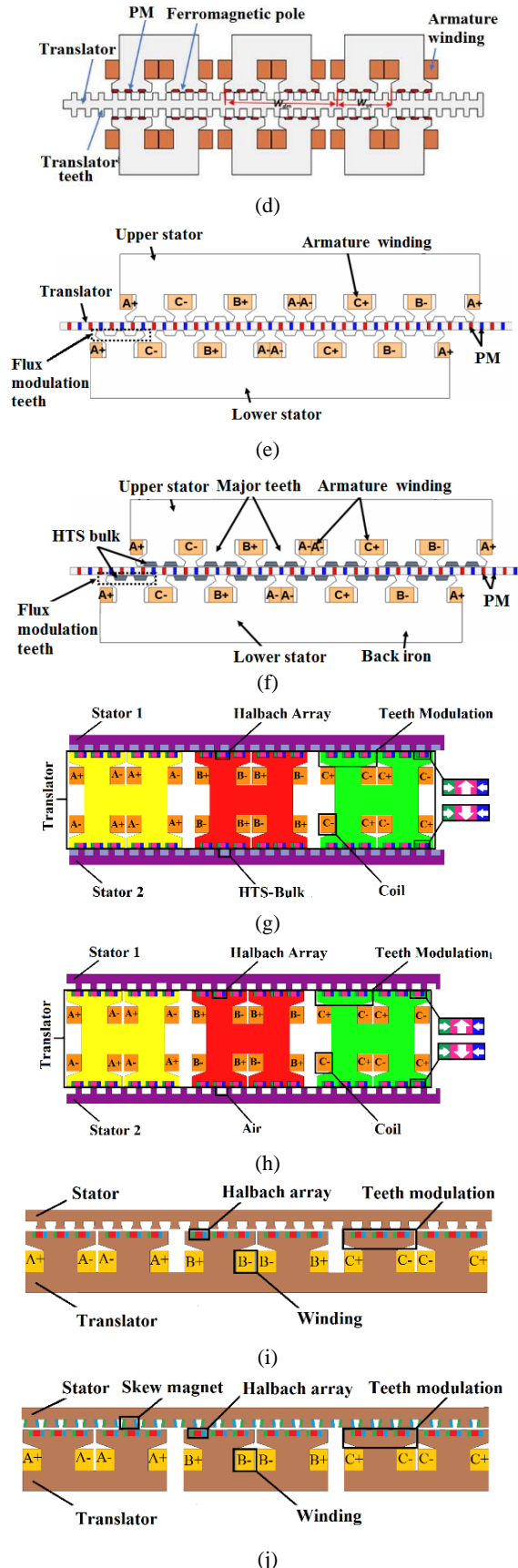


Figure. 11. Similar structures of the vernier machine, (a) A model [11], (b) B model [11], (c) C model [10], (d) D model [10], (e) E model [13], (f) F model [13], (g) G model [12], (h) H model [12], (i) I model [15], (j) J model [15], (k) K model [14], (l) L model [14],

It shows that the thrust force in the proposed vernier hybrid PM machine has been increased by 27%. In addition, ripple of thrust force for PM machine can be obtained by [17]:

$$F_r = \frac{F_{\max} - F_{\min}}{F_{\text{avg}}} \times 100\% \quad (10)$$

where, F_{\min} , F_{\max} and F_{avg} are the minimum, maximum and average amount of the thrust force respectively. According to Equation (10), ripple of the proposed vernier hybrid PM machine reduces by 5%. Moreover, detent forces in both machines are approximately the same. For a better comprehension, the similar structures of the vernier machine which were explained in the introduction have been depicted in Figure 11. In addition, performances of the similar structures compared to the proposed and prototype vernier PM machine are presented in Table 2.

TABLE 2. Performance comparison.

	PM flux (RMS)	Induced voltage (Max)	Inductance (Avg)	Thrust force (Avg)
Unit	wb	V	mH	N
A model	-	48	15.97	740
B model	-	59	16.3	818
C model	0.41	129	-	4300
D model	0.49	167	-	4950

E model	0.02	34.1	34.8	172
F model	0.036	61.8	29.9	417
G model	0.27	112	23	601
H model	0.2	88	32	448
I model	0.014	16.3	18.4	1780
J model	0.019	23.7	18.1	1860
K model	0.0125	7.9	18	196
L model	0.016	9.5	17	220
Proposed model	0.049	34	16	2300
Prototype model	0.029	26	35	1800

4. CONCLUSION

This paper proposes a linear vernier machine with the concentrated winding and skew, and halbach PM located on the translator and stator respectively. In the proposed vernier hybrid PM machine by halving the structure and choosing the right magnetic gear ratio, and shape of teeth and magnet, performance of the proposed vernier hybrid PM machine increased remarkably. Moreover, the proposed vernier hybrid PM machine is lighter and cheaper than the prototype vernier PM machine because of the halving structure. Adding PM as skew structure on the teeth of translator causes flux density in the yoke and teeth of the proposed vernier hybrid PM machine be higher than the prototype vernier PM machine. Therefore, RMS value of PM flux of the proposed vernier hybrid PM machine can achieve 0.049 Wb, compared with 0.029 Wb from the prototype vernier PM machine —i.e., 68% higher. As induced voltage is derivation of PM flux, induced voltage increases with increasing the value of PM flux. The peak of induced voltage in the proposed vernier hybrid PM machine can achieve 34 V, compared with 26 V from the prototype vernier PM machine —i.e., 30% higher. Since volume of copper is halved in the proposed vernier hybrid PM machine, self-inductance in the proposed machine diminishes remarkably. Self-inductance in the proposed vernier hybrid PM machine has reduced from 34 mH to 16 mH —i.e., 55% lower. Mutual-inductance in both structures, as all phases are separated, is near zero. This leads to both machines have excellent capacity for fault tolerance. Power factor in PM vernier machine increases with increasing the PM flux and reducing the self-inductance. Since self-inductance in the proposed vernier hybrid PM machine is lower than the prototype vernier PM machine, and PM flux in the proposed vernier hybrid PM machine is higher than the prototype vernier PM machine, the power factor in the proposed vernier hybrid PM machine

is higher than the power factor in the prototype vernier PM machine. The average thrust force in the proposed vernier hybrid PM machine and the prototype vernier PM machine is 1850 N and 1450 N respectively, which shows that the thrust force in the proposed vernier hybrid PM machine increases by 27%. Ripple of thrust force in the proposed vernier hybrid PM machine is reduced by 5% compared to the prototype vernier PM machine by skewing PM and teeth which ultimately cause the proposed vernier hybrid PM machine to be suitable for wave energy converters.

5. REFERENCES

1. Nazir, C.P., "Solar Energy for Traction of High Speed Rail Transportation: A Techno-economic Analysis", *Civil Engineering Journal*, Vol. 5, No. 7, (2019). DOI: 10.28991/cej-2019-03091353.
2. Bayani, R., Farhadi, M., Shafaghat, R., and Alamian, R., "Experimental Evaluation of IRWEC1, a Novel Offshore Wave Energy Converter", *International Journal of Engineering Transactions C: Aspects*, Vol. 29, No. 9, (2016), 1292-1299.
3. Falnes, J., "A review of wave-energy extraction", *Marine Structures*, Vol. 20, No. 4 (2007), 185-201.
4. M. A. Mueller et al., "Experimental tests of an air-cored P.M tubular generator for direct drive wave energy converters", in IET Conference Publications, (2008). DOI:10.1049/cp:20080621.
5. López, I., Andreu, J., Ceballos, S., Martínez De Alegria, I. and Kortabarria, I., "Review of wave energy technologies and the necessary power-equipment", *Renewable and Sustainable Energy Reviews*, Vol. 27, (2013), 413-434.
6. C. A. Oprea, C. S. Martis, F. N. Jurca, D. Fodorean, and L. Szabó., "Permanent magnet linear generator for renewable energy applications: Tubular vs. four-sided structures", in 3rd International Conference on Clean Electrical Power: Renewable Energy Resources Impact, ICCEP 2011, (2011), 588–592.
7. Rahman, M., Ong, Z.C., Julai, S., Ferdaus, M.M., and Ahamed, R., "A review of advances in magnetorheological dampers: their design optimization and applications", *Journal of Zhejiang University SCIENCE A*, Vol. 4, No. 12, (2017). DOI:10.1631/jzus.A1600721.
8. Moradi CheshmehBeigi, H., "Slotless tubular PM generator with dual quasi-Halbach magnetized PM Array: Analytical and numerical magnetic field analysis", *International Journal of Numerical Modelling: Electronic Networks, Devices and Fields*, Vol. 33, No. 2 (2019). DOI:10.1002/jnm.2569.
9. Hemmati, R., and Rahideh, A., "Optimal design of slotless tubular linear brushless PM machines using metaheuristic optimization techniques", *Journal of Intelligent & Fuzzy Systems*, Vol. 32, No. 1, (2017). 351-362. DOI:10.3233/JIFS-151847.
10. Almoraya, A.A., Baker, N.J., Smith, K.J. and Raihan, M.A.H., "Development of a double-sided consequent pole linear vernier hybrid permanent-magnet machine for wave energy converters", in 2017 IEEE International Electric Machines and Drives Conference, IEMDC 2017, (2017). DOI:10.1109/IEMDC.2017.8002157.
11. Almoraya, A.A., Baker, N.J., Smith, K.J., and Raihan, M.A.H., "Design and Analysis of a Flux-Concentrated Linear Vernier Hybrid Machine with Consequent Poles", *IEEE Transactions on Industry Applications*, Vol. 55, No. 5, (2019), 4595-4604. DOI:org/10.1109/TIA.2019.2918499.
12. Ardestani, M., Arish, N. and Yaghobi, H., "A new HTS dual

- stator linear permanent magnet Vernier machine with Halbach array for wave energy conversion", *Physica C: Superconductivity and its Applications*, Vol. 567, No. 12, (2020). p.1353593. DOI:10.1016/j.physc.2019.1353593.
13. Baloch, N., Khaliq, S. and Kwon, B., "HTS dual-stator spoke-type linear vernier machine for leakage flux reduction", *IEEE Transactions on Magnetics*, Vol. 53, No. 11, (2017), 1-4.
 14. Arish, N., Yaghobi, H. and Teymoori, V., "Optimization and Comparison of New Linear Permanent Magnet Vernier Machine", in 27th Iranian Conference on Electrical Engineering (ICEE). (2019), 657-661.
 15. Arish, N., Teymoori, V., Yaghobi, H. and Moradi, M., "Design of New Linear Vernier Machine with Skew and Halbach Permanent Magnet for Wave Energy Converter", 34 th P ower System Conference (PSC), (2019).
 16. Bian, F. and Zhao, W., "A new dual stator linear permanent-magnet vernier machine with reduced copper loss", *AIP Advances*, Vol. 7, No. 5, (2017). DOI:10.1063/1.4978589.
 17. Zhao, W., Zheng, J., Wang, J., Liu, G., Zhao, J. and Fang, Z., "Design and analysis of a linear permanent-magnet vernier machine with improved force density", *IEEE Transactions on Industrial Electronics*, Vol. 63, No. 4, (2016), 2072-2082.
 18. Nematsaberi, A. and Faiz, J., "A Novel Linear Stator-PM Vernier Machine With Spoke- Type Magnets", *IEEE Transactions on Magnetics*, Vol. 54, No. 11, (2018), 1-5.
 19. Shafaie, R. and Kalantar, M., "Comparison of theoretical and numerical electromagnetic modeling for HTS synchronous generator", *IEEE Transactions on Applied Superconductivity*, Vol. 25, No. 1, (2015), 1-7.
 20. Ainslie, M.D. and Fujishiro, H., "Modelling of bulk superconductor magnetization", *Superconductor Science and Technology*, Vol. 27, No. 5, (2015) 053002. DOI:10.1088/0953-2048/28/5/053002.
 21. Grilli, F., Brambilla, and Martini, L., "Modeling high-temperature superconducting tapes by means of edge finite elements", *IEEE Transactions on Applied Superconductivity*, Vol. 17, No. 2, (2007) 3155-3158.
 22. A. N. Patel and B. N. Suthar, "Cogging torque reduction of sandwiched stator axial flux permanent magnet brushless dc motor using magnet notching technique", *International Journal of Engineering Transaction A: Basics*, Vol. 32, No. 7, (2019), 940-946.
 23. Liu, G., Ding, L., Zhao, W., Chen, Q. and Jiang, S., "Nonlinear equivalent magnetic network of a linear permanent magnet vernier machine with end effect consideration" *IEEE Transactions on Magnetics*, Vol. 54, No. 1, (2018). DOI:10.1109/TMAG.2017.2751551.
 24. Li, D., Qu, R. and Lipo, T.A., "High-power-factor vernier permanent-magnet machines", *IEEE Transactions on Industry Applications*, Vol. 50, No. 6, (2014), 3664-3674.
 25. Moradi Cheshmeh Beigi, H., "Design, optimization and FEM analysis of a surface-mounted permanent-magnet brushless DC motor", *International Journal of Engineering, Transaction B: Applications*, Vol. 31, No. 2, (2018), 339-345.
 26. A. N. Patel and B. N. Suthar, "Cogging torque reduction of sandwiched stator axial flux permanent magnet brushless dc motor using magnet notching technique", *International Journal of Engineering Transaction A: Basics*, Vol. 32, No. 7, (2019), 940-946.

Persian Abstract

چکیده

امروزه اهمیت استفاده از انرژی های تجدید پذیر دو برابر شده است ، زیرا انرژی های غیرقابل تجدید تا چند سال آینده تمام می شوند. هدف از این مقاله ارائه یک ساختار ماشین ورنبر خطي جدید است که برای به دام انداختن انرژی موج و بهبود بخشیدن عملکرد ماشین ورنبر اولیه طراحی شده است. با نصف کردن ماشین ورنبر ارایه شده و اصلاح ضرب گیریکس و تغییر شکل آهنربای دائمی و شکل دنده، عملکرد ماشین ورنبر اولیه افزایش یافته است. این نوآوری باعث می شود ماشین ورنبر ارایه شده سبکتر ، اقتصادی تر و کارآمدتر از ماشین ورنبر اولیه باشد. علاوه بر این ، پارامترهای اصلی ماشین ورنبر ارایه شده نسبت به ماشین ورنبر اولیه بهبود یافته است، به طوری که در ماشین ورنبر ارایه شده، ولتاژ القابی، شار آهنربای دائمی و نیروی رانش به ترتیب 27% ، 20% و 68% افزایش یافته است. همچنین، دیبل نیروی رانش 4% کاهش یافته است و اندوکتانس خودی 55% تقلیل پیدا کرده است. تمام تجزیه و تحلیلها در شرایط مشابه با روش المان محدود با استفاده از نرم افزار انسیس مکسول انجام شده است.
